SERA
Seismology and Earthquake Engineering
Research Infrastructure Alliance for Europe

INTERNAL REPORT

1 Key Results for JRA2/JRA3: Characterizing the Activity Rates of Induced and Natural Earthquakes

Work package	WP24, JRA2: Characterizing the activity rates of induced and natural earthquakes
Lead	GFZ-Potsdam
Authors	Anne Strader, GFZ-Potsdam; Fabrice Cotton, GFZ-Potsdam; Danijel Schorlemmer, GFZ-Potsdam
Reviewers	[Name, Institution]
Approval	[Management Board]
Status	[Draft/final]
Delivery deadline	[DD.MM.YYYY]
Submission date	[DD.MM.YYYY]
Intranet path	[DOCUMENTS/DELIVERABLES/File Name]

Table of Contents

2 Task 24.1: Open-source toolbox for seismicity analysis

PyMap, currently under development, is an open-source Python/Qt-based toolbox for computation of earthquake statistics. Expanding upon the capabilities of ZMAP, PyMap provides a unified API for seismicity analysis on different scales, including global and regional earthquakes, induced earthquakes or earthquakes occurring in mining environments, and acoustic emission events in laboratory samples. PyMap will also accommodate multiple types of study grids, including global grids with varying tesselation procedures, Mercator-style simple grids, and rock laboratory dimensions.

2.1 ZMAP 7.0 Seismicity toolbox

Concurrently, ZMAP Version 7 is under development, compatible with versions of MATLAB from 2018 onward. Current ZMAP developments will facilitate the implementation and transfer of existing modules to PyMap and allow crosschecking of PyMap and ZMAP tools.

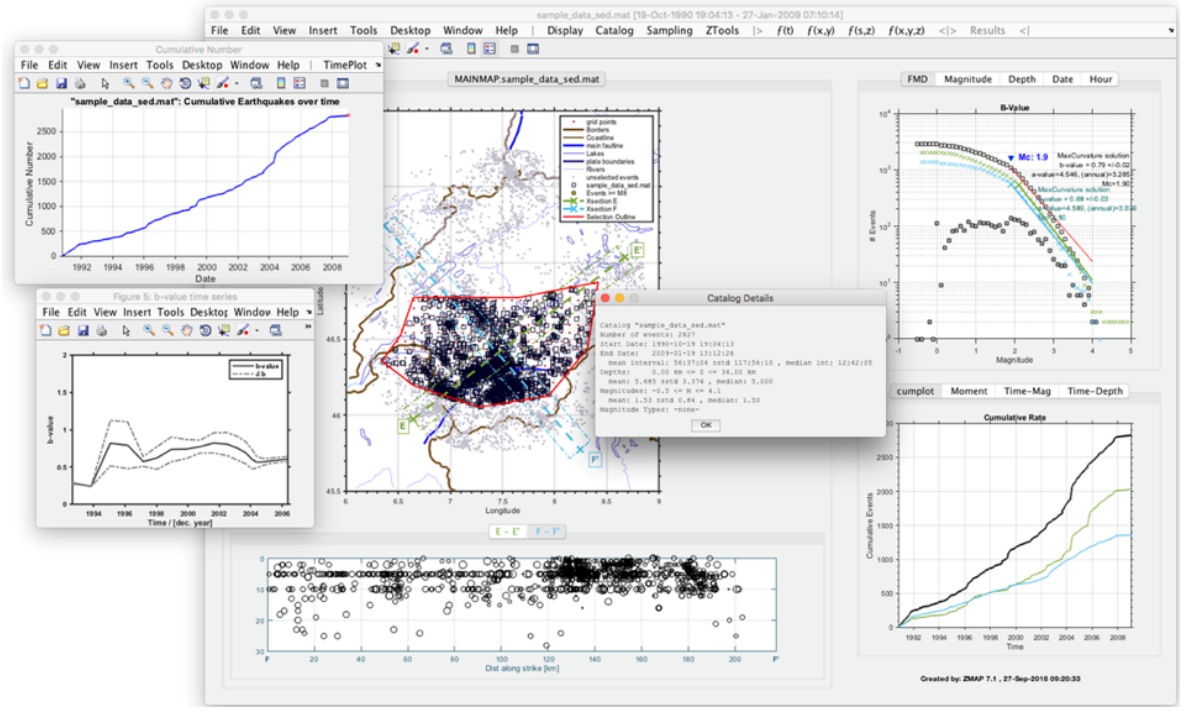

Figure 1. Sample ZMAP 7 interface

Earthquake catalogues are probably the most fundamental products of seismology and remain arguably the most useful for tectonic studies. Modern seismograph networks can locate upwards of a hundred thousand earthquakes annually, providing a continuous and sometime overwhelming stream of earthquake locations. ZMAP is a set of tools driven by a graphical user interface (GUI), designed to help seismologists analyse catalogue data. ZMAP is primarily a research tool suited to the evaluation of catalogue quality and to addressing specific hypotheses; however, it can also be useful in routine network operations. ZMAP was first published in 1994, with the last major release, version 6.0, in 2001.

ZMAP 7 depends upon MathWorks MATLAB® R2018a or higher, and will work on Windows, MacOSX and Linux operating systems. Additionally, the following MATLAB toolboxes must be installed:

- Mapping Toolbox
- Statistics and Machine Learning Toolbox
- Parallel Computing Toolbox [optional, enables parallel computing]

ZMAP is currently hosted on GitHub at: https://github.com/CelsoReyes/zmap7, with links to the download available from the main SED website http://www.seismo.ethz.ch/en/research-and-teaching/products-software/software/ZMAP/ .

ZMAP 7 represents a major reworking of ZMAP 6.0. Every aspect of ZMAP has been modified -- from the user interface through the data representations within the program-- according the following goals:

- Make ZMAP compatible with modern MATLAB installations. MATLAB has evolved far beyond the version for which ZMAP 6.0 was designed and in several cases broke backwards compatibility. In the intervening years, new, robust techniques for performing object oriented design have driven changes to the graphics system underpinning the user interface, as well as to the language itself.
- Make it easier to add additional functionality. By leveraging functions and classes, future users inherit a consistent interface that allows the easy addition powerful analysis routines with very little code duplication.
- Make the user interfaces more consistent and interactive. Frequently recurring user-interfaces (e.g. dialog boxes) were once generated at a low level in each routine and differed wildly between routines. Now, the most common of these have been consolidated and a method for consistently generating them has been added.
- Make code more robust. Originally, ZMAP code consisted of a large selection of scripts that operated on global variables and made assumptions about the GUI's state. Callbacks, a primary component of GUIs, were string-based scripts that were "invisible" to the MATLAB syntax checker. Now, scripts have been extracted into individual functions, allowing for better code reuse and allowing the languages validation tools to efficiently function.
- Make existing code more readable and maintainable. This has involved reducing code duplication through the use of consolidated helper functions and classes. Home-grown functionality has been removed in favor of standard toolbox functions, further reducing the need for maintenance. All entities (classes, functions, and variables) are being renamed to reduce the cognitive burden of maintainers to follow.
- Simplify access to event catalogues. ZMAP can load catalogue data directly from FDSN Event Webservice websites in addition to a variety of file formats or local variables.

While optimizing for speed was not a goal in itself, the previous points all contribute to the ease of finding and fixing inefficiencies resulting from naïve algorithm choice or inefficient porting from other languages (esp. FORTRAN). Additionally, several algorithms may take advantage of parallel processing capabilities.

ZMAP 7 is currently in alpha release stage while its functionality continues to evolve. However, the basic functionality is in place and already allows one to easily explore earthquake catalogs. When users encounter bugs or user-unfriendly behaviour, they are encouraged to report them to the ZMAP developer(s) via the GitHub issue reporting system, conveniently accessible from within the ZMAP help menu. These issues are visible by both the program maintainer(s) and the community and becomes a touchstone for understanding which aspects of ZMAP are important to the community .

Table 1
Learning Goals and Their Associated Jupyter Notebooks

	Learning Goal	Notebook Title
1	Python data types	Introduction to Python
		Introduction to reading data and plotting using Pandas
2	Import and export data	Introduction to reading data and plotting using Pandas
		Introduction to plotting data as a heat map
3	Basic figure making	Introduction to reading data and plotting using Pandas
		Introduction to plotting data as a heat map
		Introduction to scatter plots and histograms
4	Histograms	Introduction to scatter plots and histograms
5	Map making	Creating a map in cartopy and plotting data on it
		Plotting focal mechanisms on a cartopy map
		Plotting a pretty map using cartopy
		Plotting heat map data on a map using cartopy
		Maps for unshaped data using cartopy
6	Exploratory data analysis	Introduction to plotting data as a heat map
		Introduction to scatter plots and histograms
		Creating a map in cartopy and plotting data on it
		Plotting heat map data on a map using cartopy
7	Jupyter Notebooks	All notebooks

Instead of having a linear progression (notebook 1, notebook 2, notebook 3, etc.), we assign Notebooks to learning goals to aid in the modularity of the materials.

Figure 2. Table 1 from Aiken et al. (2018), summarizing the main learning goals and associated Jupyter notebooks of their Python library for earthquake statistics computation and data visualization.

Reference:

Wiemer, S., 2001. A software package to analyze seismicity: ZMAP. Seismological Research Letters, 72(3), pp.373-382 https://doi.org/10.1785/gssrl.72.3.373

2.2 Computational chain code development and educational tools

PyMap code development has recently begun, focusing on the statistical seismology computational chain from input data (earthquake catalogs) to data quality analysis to computation of earthquake-catalog statistical parameters and results visualization. Examples of data quality measures to be implemented include recording completeness at various magnitude thresholds, temporal variations in seismicity rates, and data contamination. Tools to compute statistical parameters such as seismicity rates and b-values are already available as a Python library developed by Aiken et al. (2018). The corresponding Jupyter notebooks, which are freely available, provide tutorials for statistical seismicity computations intended for use by seismology students. Figure 1 provides a list of the notebooks and their associated learning goals, which focus on data analysis using the Pandas library and visualization of earthquake statistics such as spatiotemporal b-value variations. The notebooks were successfully applied in a Master's level PSHA course at the University of Potsdam, providing exposure to mapmaking and statistical analysis using Python to students with little to no programming experience. In the future, the authors plan to develop a module for seismic-waveform data analysis through the ObsPy toolbox.

3 Task 24.2: Characterization of earthquakes sequences and background-seismicity rates

Our starting point has been the previous analysis performed to develop the SHARE hazard model (Woessner et al., 2015). We have analyzed the methods used to evaluate the background (i.e. declustered) seismicity rates during this project (Figure 2). The rates were determined primarily from earthquake-catalog data using the SHARE European Earthquake Catalogue (SHEEC). After declustering the earthquake catalog using the windowing-approach of Burkhard and Grünthal (2009), only 8000 of the original 30,000 earthquakes remain for background seismicity rate characterization. As a result, seismicity rates and magnitude frequency distributions are estimated based on few earthquakes, and must be estimated using expert opinion for low-seismicity zones. Nearly half of the 432 area source zones contain fewer than 10 earthquakes, necessitating further investigation into the impact of few available earthquake data on the stability of background seismicity characterization.

In this task, we considered the following three factors: 1) analysis of the impact of different types of declustering and declustering "correction" methods on the background seismicity rate, 2) estimation of the epistemic uncertainty on the background seismicity rates, and 3) analysis of the time-dependency beyond well-known short-term seismic clustering.

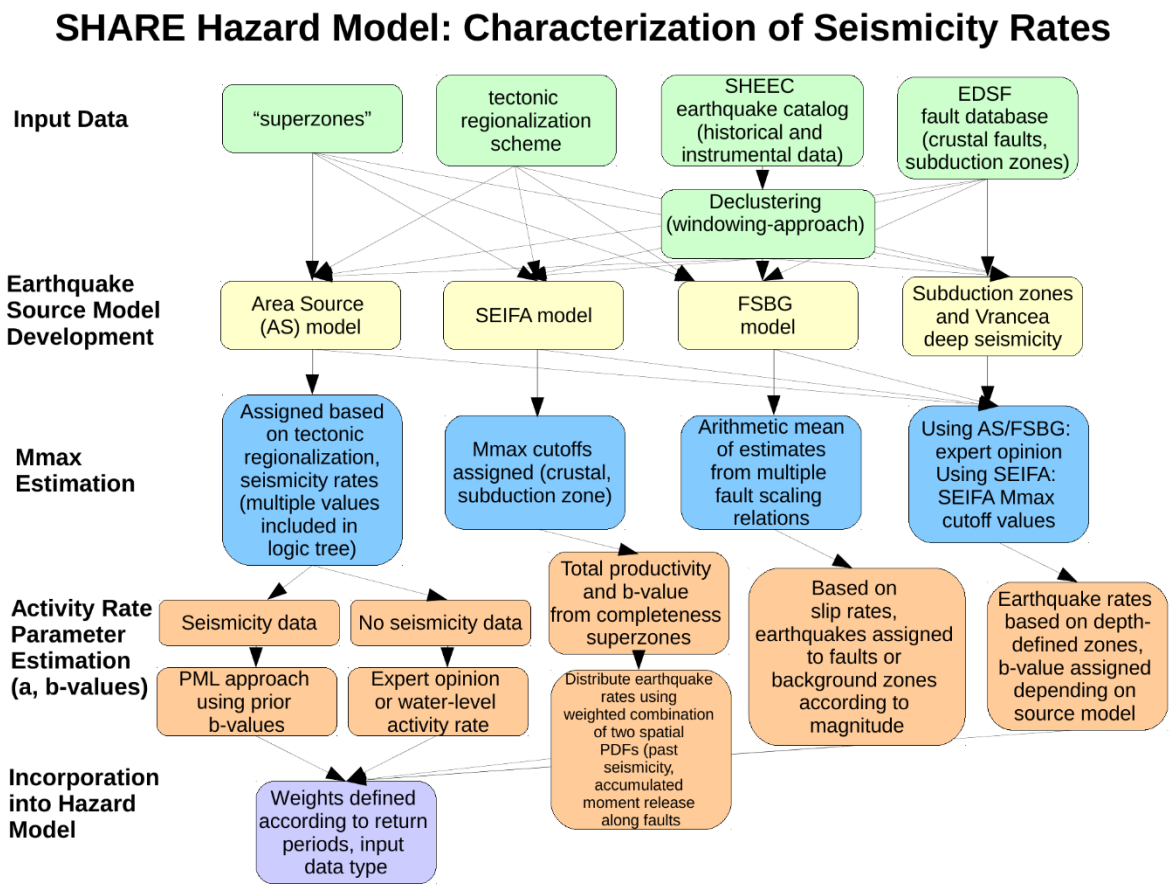

Figure 3. Flowchart of seismicity rate characterization for the SHARE hazard model. In the case of the area source model, often too few earthquakes are available to constrain local b-value variations using data-driven methods, therefore these values are often based on expert opinion.

3.1 Seismicity rates in low-seismicity zones

Because PSHA is based on the assumption that the seismicity rate follows a Poisson distribution, dependent events must be removed from the earthquake catalog before calculating background seismicity rates. The choice of declustering method is largely subjective, as there exists no physical definition of an "independent" vs. "dependent" earthquake. As shown in Figure 3, in which five declustering methods have been compared for the Advanced National Seismic System (ANSS) earthquake catalog, the choice of declustering method has considerable impact on earthquake rates and numerous methods fail to completely remove aftershock sequences. Additionally, varying earthquake-catalog time scales are not taken into account when applying declustering methods.

To investigate the impact of available earthquake catalog data on the stability of the magnitude-frequency distribution, Anne Strader (GFZ-Potsdam) used varying time windows of the Japan Meteorological Agency (JMA) earthquake catalog to emulate earthquake catalogs for zones with varying amounts of earthquake data (Figure 4). The impacts of time intervals (3-month, 6-month, 1-year, 2-year and 5-year), completeness magnitudes (2.5, 3.0, 3.5, 4.0), and declustering (using the Gardner-Knopoff method) on the b-value and its stability were investigated. For consecutive time intervals, a slight increase in b-value was observed for shorter time intervals and greater completeness magnitudes, but the mean b-value remained close to 1. Because the GK declustering method primarily removes smaller earthquakes (Marzocchi and Taroni, 2014), the mean b-value was reduced to 0.5 after declustering the earthquake catalog, causing larger b-value variations with respect to magnitude completeness and time interval durations. This result is consistent with large b-value variations observed in the SHARE hazard model area source zones, where prior b-value estimates were updated for each zone using available earthquake catalog data. The observed impact of declustering on b-values even for large catalogs (i.e. five-year time intervals) indicates that b-values may not be robust for the area source zones or tectonic "superzones" within the SHARE region.

The number of earthquakes necessary to constrain the b-value is currently under debate within the seismic hazard community. A key question for SERA is whether SHARE superzones and area source zones contain sufficient earthquake data to reliably constrain local spatial b-value variations. Strader investigated the impact of earthquake data amounts on b-

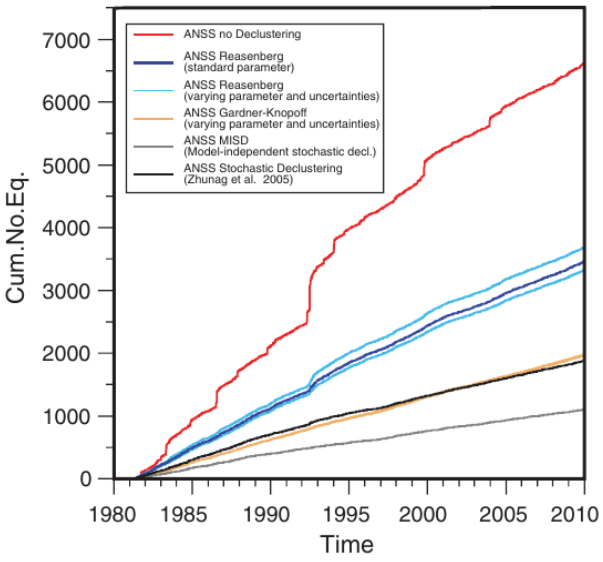

Figure 4 Cumulative numbers of earthquakes for multiple declustering methods applied to the ANSS earthquake catalog. In addition to large variations.

Fabric
Delete

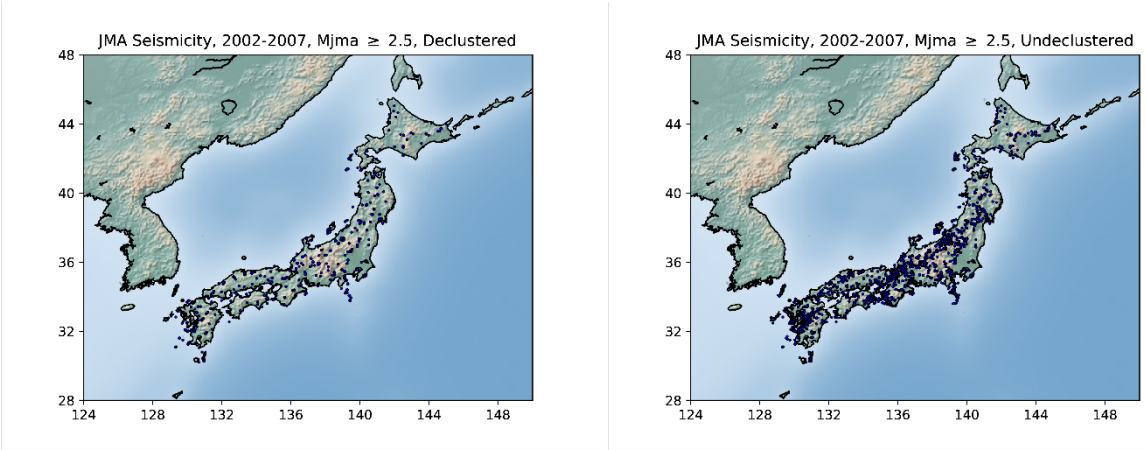

Figure 5. Seismicity maps (left, undeclustered; right, declustered) for the JMA earthquake catalog within the Mainland region from 2002-2007, with a magnitude completeness of $M_{jma} \geq 2.5$.

value stability by calculating the b-value for consecutive JMA subcatalogs containing 50 and 200 earthquakes. Although a quantity of 200 earthquakes is generally accepted as sufficient to constrain the b-value of a study region, variations of approximately ±0.3 and ±0.03 were observed for undeclustered and declustered subcatalogs,

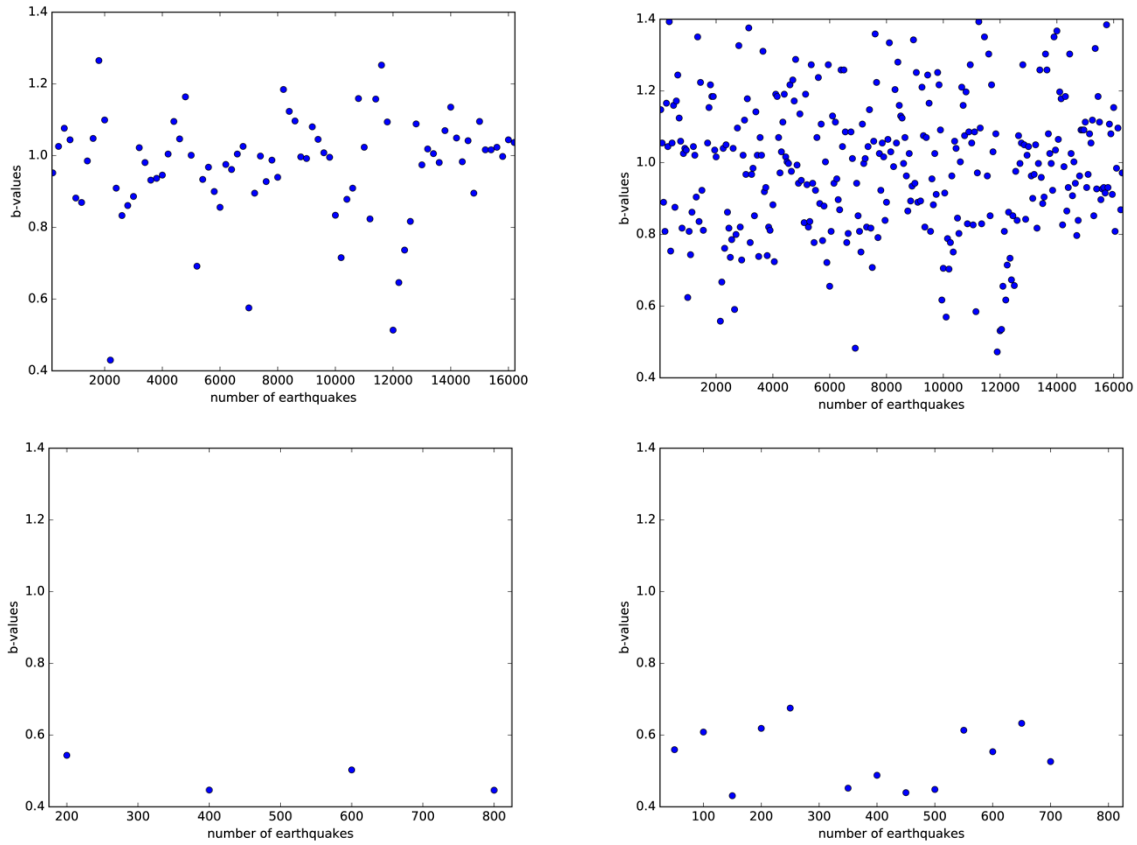

Figure 6. Temporal variations in b-values for consecutive declustered (bottom row) and undeclustered (top row) earthquake catalogs containing 200 earthquakes (left column) and 50 earthquakes (right column) each. The mean b-value for the declustered catalog is substantially lower than for the undeclustered catalog due to the tendency of the GK declustering method to primarily remove smaller earthquakes, while without declustering the b-value displays large temporal variations for both the 50-earthquake and 200-earthquake catalogs.

respectively (Figure 5). For subcatalogs containing 50 earthquakes each, b-value variations increased to ±0.4 for undeclustered and ±0.1 for declustered subcatalogs. Almost half of area source zones contain fewer than 10 earthquakes, reinforcing that robust b-value spatial variations may not be constrained given currently-available European earthquake-catalog data.

Danijel Schorlemmer (GFZ-Potsdam) investigated whether earthquake catalogs tend to follow a Poisson distribution after being declustered. Based on an analysis of temporal seismicity rate variations for the declustered JMA and GeoNet (New Zealand) earthquake catalogs, he found that both catalogs did not exhibit Poisson behavior (Figure 6), particularly during years prior to increased seismic network density, for example the availability of Hi-Net data in the JMA catalog after 2002.

Temporal variations in b-values for consecutive declustered (bottom row) and undeclustered (top row) earthquake catalogs containing 200 earthquakes (left column) and 50 earthquakes

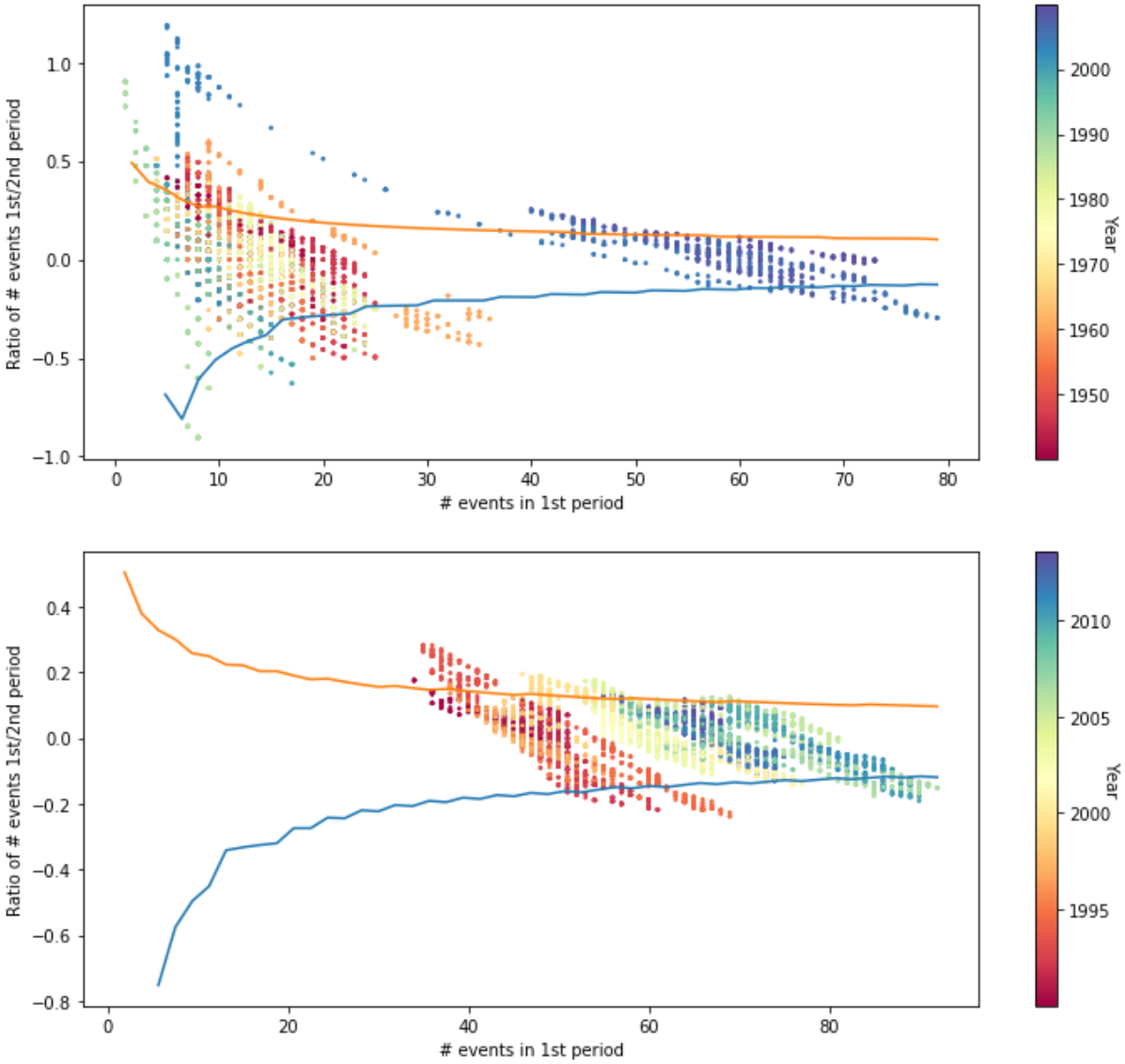

Figure 7. Plots of inter-event time ratios for the declustered JMA (top) and GeoNet (bottom) earthquake catalogs. Although a greater proportion of ratios are within the Poisson distribution 0.05 significance level for recent years, neither catalog displays Poisson behavior after declustering.

(right column) each. The mean b-value for the declustered catalog is substantially lower than for the undeclustered catalog due to the tendency of the GK declustering method to primarily remove smaller earthquakes, while without declustering the b-value displays large temporal variations for both the 50-earthquake and 200-earthquake catalogs.

3.2 Impact of declustering methods on earthquake sequences and ground-motion exceedance probabilities

Because earthquake catalogs do not contain sufficient data to constrain long-term clustering properties, using an undeclustered earthquake catalog as input in seismic hazard analysis results in spatial bias, where earthquake and hazard rates are overestimated in regions with recent seismicity clustering (Marzocchi and Taroni, 2014). However, traditional declustering methods in PSHA such as the GK method result in underestimation of seismic hazard. At a given site, the peak ground acceleration (PGA) caused by an aftershock is likely to exceed that of the mainshock given a large ratio between the distance from the site to the mainshock and from the site to the aftershock. Therefore, smaller earthquakes that may contribute significantly seismic hazard are often removed from earthquake catalogs prior to hazard calculation. Marzocchi and Taroni (INGV) observed that, given an exceedance rate equal to or lower than 0.1 and nonnegligible ground-motion parameter thresholds, earthquake rates must not necessarily follow a Poisson distribution in order for the exceedance probabilities to follow a Poisson distribution. They concluded that declustering is necessary only due to spatial bias, and introduced a "correction" to ensure that total declustered seismicity rates in a region are equal to the rate observed in the original earthquake catalog. Figure 7 compares seismic hazard maps for Italy without declustering, after declustering, and after "correcting" for declustering. Large differences in PGA within central and southern Italy indicate that short-term seismic clustering significantly impacts long-term seismic hazard.

Angela Stallone (INGV) and Warner Marzocchi recently investigated the impact of tectonic environment on statistical properties of declustered earthquake catalogs. They compared the cumulative number of earthquakes over the number of earthquakes per cluster, cluster

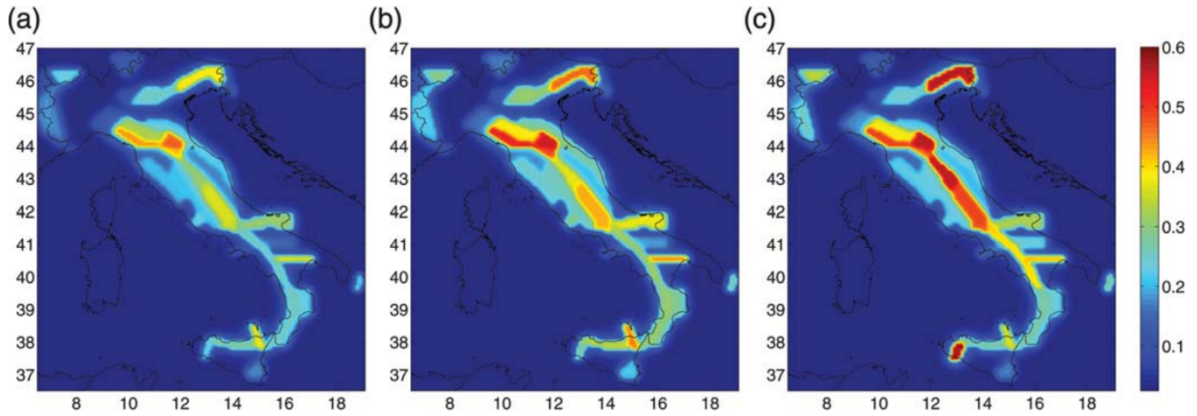

Figure 8. PGA maps (10% exceedance probability in 50 years) for Italy using a) declustered seismicity rates, b) "corrected" declustered seismicity rates, and c) undeclustered seismicity rates (Marzocchi and Taroni, 2014). In central and southern Italy, short-term earthquake clustering substantially increases exceedance probabilities, while underestimation of the hazard through declustering can be observed by comparing the hazard maps based on corrected and uncorrected declustered seismicity rates.

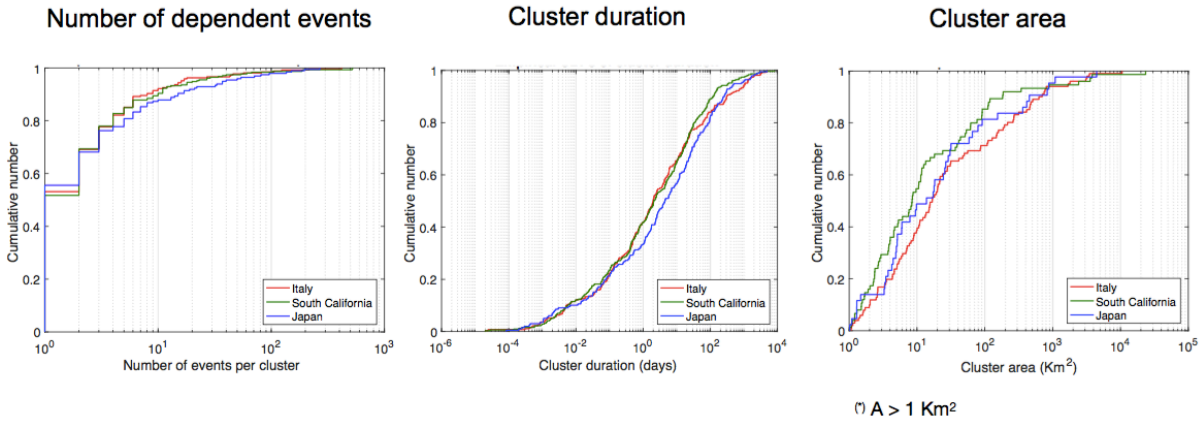

Figure 9. Cumulative earthquake numbers with respect to numbers of earthquakes per cluster, cluster duration, and cluster area for Italy, southern California and Japan (Stallone and Marzocchi, in prep). No significant differences in clustering properties are observed within the three regions, suggesting that the same declustering method can be applied to all tectonic domains.

duration, and cluster area, finding no significant difference in earthquake numbers between catalogs for Italy, southern California and Japan (Figure 8). This suggests that seismic sequences in distinct tectonic domains are not significantly different, and the same declustering method can reliably be applied to different tectonic environments.

3.3 Characterization of earthquake clusters with spatially-varying ETAS models

To incorporate the effects of short-term earthquake clustering properties in spatial seismic hazard variations, Shyam Nandan (ETH Zürich) developed an Epidemic Type Aftershock Sequence (ETAS) seismicity model with spatially-varying ETAS parameters (Nandan et al., 2017). Introducing an efficient method for parameter estimation using the expectation maximization (EM) algorithm and spatial Voronoi tessellation ensembles, Nandam found that earthquake triggering is dominated by small earthquakes within the Regional Likelihood Earthquake Model (RELM) California region (Figure 9). Furthermore, the branching ratio (the efficiency of earthquake triggering by previous events) was positively correlated with surface heat flow, indicating that the crust within regions of elevated heat flow is closer to the local critical stress threshold. This is supported by evidence of remote dynamic triggering in areas with geothermal and/or volcanic activity, where the branching ratios are relatively large. These results imply that seismicity rate models based on Coulomb stress changes should account for secondary static stress changes caused by smaller earthquakes, as well as far-field triggering through fluid-induced activation.

Seismicity forecasts generated from the optimal ETAS model, an ensemble of ETAS models with no significant log-likelihood deviation from the best ETAS model at the 0.05 significance level, were pseudo-prospectively evaluated against smoothed seismicity models for California (for example, Helmstetter et al., 2007). The ETAS ensemble model outperformed smoothed-seismicity models solely based on declustered earthquake-catalog data, suggesting that the ETAS model has the potential to reliably capture triggering properties of background earthquakes. The ETAS model will be prospectively tested within the Collaboratory

for the Study of Earthquake Predictability (CSEP) and is currently being considered as an alternate background seismicity model for Europe in the next iteration of the European seismic hazard model.

3.4 Magnitude-Independence Assumption

In earthquake forecasting as well as PSHA, it is commonly assumed that the magnitude of an earthquake is independent from past seismicity. Stallone and Marzocchi (2018, in review) compared magnitude-frequency distributions for background and triggered seismicity and investigated how seismicity variations in the space-time-magnitude domain can be used to estimate future earthquake magnitudes. Using the approach introduced by Zaliapin et al. (2008) to distinguish between triggered and background seismicity, they found that for all tested catalogs the magnitude-independence assumption was upheld, with one exception where the largest earthquakes occurred at the edge of the spatial distribution of triggered

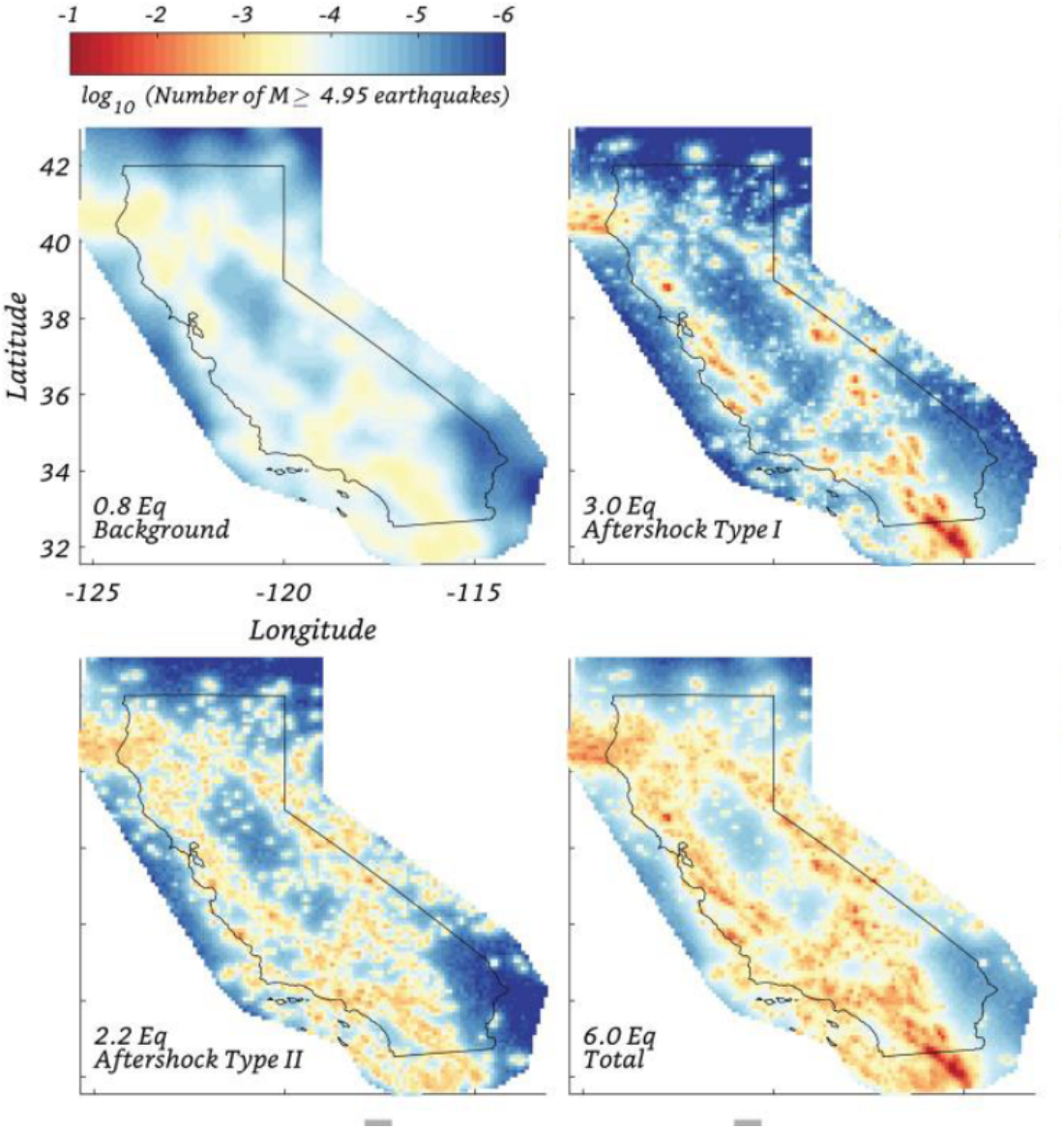

Figure 10. Background seismicity, primary and secondary aftershock triggering, and total seismicity rates for the RELM California region (Nandan et al., 2017). The optimal ETAS ensemble model indicates that smaller earthquakes are the primary contributors to future earthquake triggering, and should be taken into account in long-term seismic hazard models.

seismicity. However, previously-observed deviations from the magnitude-independence assumption are invalidated when taking into account spatiotemporal variations of the completeness magnitude.

4 Task 24.3: Time-Dependent Induced-Seismicity Models and their Dependency on Time-Varying Operational Parameters. Guidelines for Time-Dependent Hazard Evaluation

The rise in the frequency of anthropogenic earthquakes due to deep fluid injections is posing serious economic, societal, and legal challenges to many geo-energy and waste-disposal projects. Existing tools to assess such problems are still inherently heuristic and mostly based on expert elicitation (so-called clinical judgment). We have developed in Mignan et al. (2018) an adaptive traffic light system (ATLS) that is function of a statistical model of induced seismicity. It offers an actuarial judgement of the risk, which is based on a mapping between earthquake magnitude and risk. Using data from six underground reservoir stimulation experiments, mostly from Enhanced Geothermal Systems, we illustrate how such a data-driven adaptive forecasting system could guarantee a risk-based safety target. The proposed model, which includes a linear relationship between seismicity rate and flow rate, as well as a normal diffusion process for post-injection, is first confirmed to be representative of the data. Being integrable, the model yields a closed-form ATLS solution that is both transparent and robust. Although simulations verify that the safety target is consistently ensured when the ATLS is applied, the model from which simulations are generated is validated on a limited dataset, hence still requiring further tests in additional fluid injection environments.

We also have developed a Bayesian hierarchical framework to model fluid-induced seismicity (Broccardo et al., 2017). The framework is based on a non-homogeneous Poisson process (NHPP) with a fluid-induced seismicity rate proportional to the rate of injected fluid. The fluid-induced seismicity rate model depends upon a set of physically meaningful parameters, and has been validated for six fluid-induced case studies. In line with the vision of hierarchical Bayesian modeling, the rate parameters are considered as random variables. We develop both the Bayesian inference and updating rules, which are used to develop a probabilistic forecasting model. We tested the Basel 2006 fluid-induced seismic case study to prove that the hierarchical Bayesian model offers a suitable framework to coherently encode both epistemic uncertainty and aleatory variability. Moreover, it provides a robust and consistent short-term seismic forecasting model suitable for online risk quantification and mitigation.

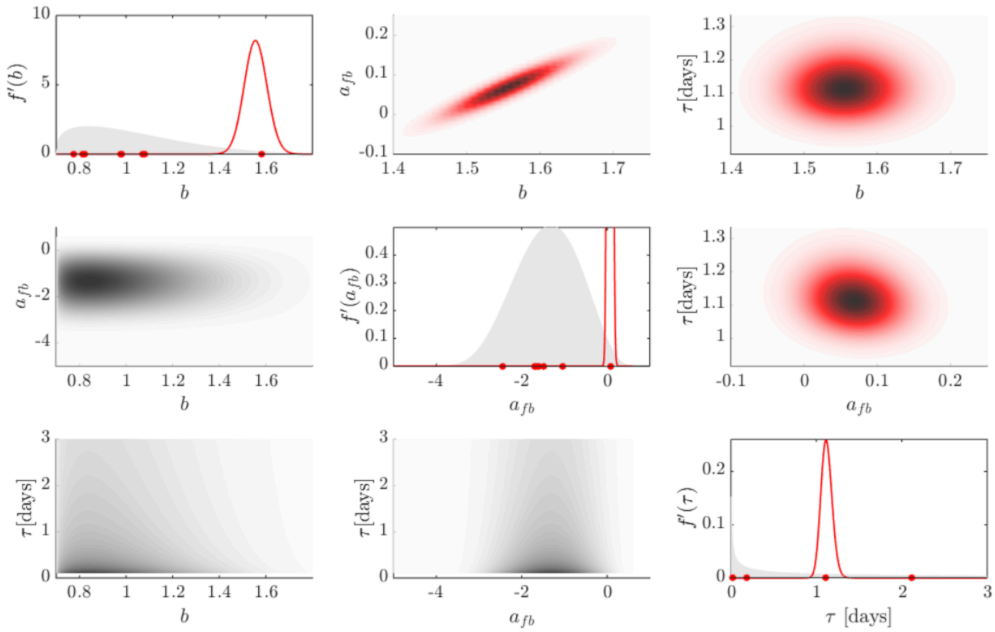

Figure 10: Prior and posterior distribution for Basel 2006 dataset: m0=0.8, time[0,12]days magnitude M_W. Diagonal: in shaded grey the prior distributions, with red lines the posterior distributions, red dots rep-resent the maximum likelihood estimators. See Broccorado et al. (2017) for details.

Similar to applying mainshock rupture length to estimate the spatial extent of an aftershock zone, Grasso et al. (2018) estimated the spatial extent of reservoir-triggering earthquakes from reservoir length. They determined that for the 26 largest impounded reservoirs in continental France, about a quarter of the reservoirs trigger M_{max} = 2.5–4.7 earthquakes within one reservoir length during a 15-year time window. Evaluated against a randomized series, they identify a robust increase in the average seismicity rate within two years within 1-3 reservoir lengths, with larger reservoirs triggering more often than smaller ones. Reservoir length is demonstrated to be more important than reservoir depth in estimating the spatial extent of induced-reservoir earthquakes, and the M_{max} for reservoir-triggered seismicity tends to remain smaller than the reservoir magnitude equivalent.

5 Task 24.4: Test-Beds for the Validation of Tools and Methodologies

The work on designing a test bed for the validation of tools and methodologies is progressing well.
Because the necessary testing and validation covers a range of different model components and application, there will not be a single test bed for all applications, but tailor one for different purposes:

1) **Test bed for seismicity analysis tools:** We are currently comparing the results when computing seismicity parameters independently with PyMap, ZMAP7 and GEM tools. So far, no major differences were observed. In a second step, we will formalize this testing by defining a specific benchmark which known properties.
2) **Testing seismicity forecasts**: Here we use the established CSEP forecast center. Schorlemmer et al. (2018) has reviewed the established methodologies for testing within CSEP, and also highlighted some of the shortcomings. Taroni et al., (2018) have used the CSEP tests of applied to Italy, for 1-day, 3 months and 5 year models, an important milestone in evaluating a fully prospective forecast test. We are currently working on extending the CSEP testing framework for non-poissonian model assumptions. These tests (Nandam et al, in preparation) illustrate that indeed modifications to the testing metrics are warranted, which will be implemented in the next few months. We also have started to work on testing the performance of the SHARE (ERSHM13) seismogenic source models again the last 10 years of independent earthquake data. The results of this test will give important constraints on the design of the seismogenioc source model of the ESHM2020 (JRA3/WP25)
3) **Testing induced seismicity forecast models**: Here we are following the approach proposed by Kiraly et al. (2017) and Kiraly et al. (2018), who have proposed a test bench for induced seismicity evaluation and multi-component ensemble modeling (Figure 11). This approach will allows to accommodate 3D seismicity distributions in the testing, a pre-requisite for induced seismicity models. The model weights can then be used also for operating real-time, adaptive traffic lights systems for induced seismicity control. We are currently setting up the testing workflow as part of a real-time system, so that all model component can be evaluated (earthquake location, magnitude assessment, seismicity forecast and performance evaluation.

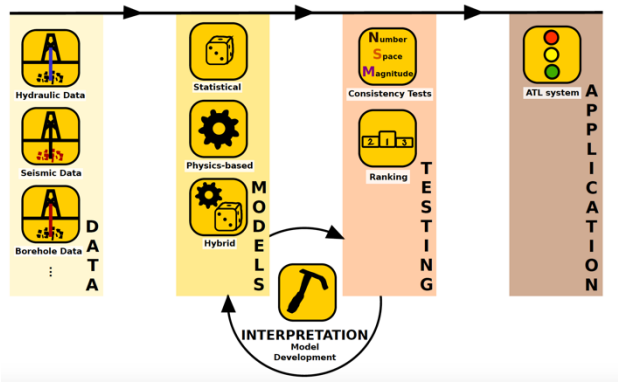

Figure 11. Proposed induced seismicity test bench (Kiraly et al., 2017).

With respect to testing data, we have prepared a important testing data set for the Grimsel underground stimulation work (Figure 11, Villiger et al, in preparation). Six hydraulic stimulation (HS) experiments were performed in a 20 x 20 x 20 m crystalline

rock volume, in which the stress state and geology was exceptionally well characterized. A standardized injection protocol was used for the six HS experiments. In total 1'000 l of water was injected in every HS experiment. Aside of the high-resolution deformation- and pressure-monitoring networks, a highly sensitive acoustic emission monitoring network was installed. Several thousand micro-seismic events were detected and subsequently located (Figure 10). This data set, once finalised, will be the primary testing data set for induced seismicity benchmarking tests in SERA

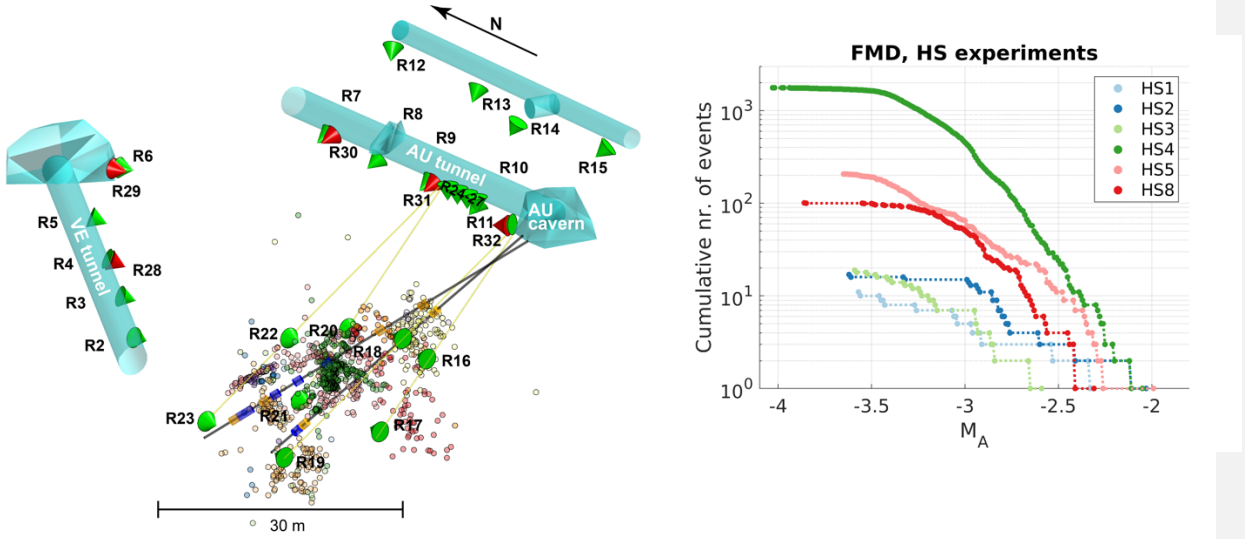

Figure 12. Left: Seismic monitoring network at Grimsel test site, consisted of 26 acoustic emission (AE) receiver (green cones) and 5 accelerometer (red cones) for calibration purposes along with all located events of the experiments. Right: Preliminary frequency-magnitude distribution of the different stimulation, showing the wide variability of the seismogenic response.

6 Task 24.5: Update and Extension of the Seismogenic Source Model

As part of the ESHM2013, an update of the Euro-Mediterranean Earthquake Catalogue (EMEC) was constructed (Fig. 13), developing magnitude scales conversions and harmonizing earthquake catalogues from across the Euro-Mediterranean region into a common catalogue of earthquakes with $M_W \geq 4$ for the period 1000 AD to 2006 (Grünthal & Wahlström, 2012). This EMEC catalogue has now been updated to include the addition of recent seismicity from the period 2007 to 2016, the results of ongoing research into historically reported events, and incorporation of new data from networks and sources not available at the time of the previous EMEC construction. This new catalogue has been presented at the EGU conference (Lammers et al., 2018) and sent to key JRA3-SERA partners (ETHZ, INGV) for revisions and suggestions in August 2018. The final version of the catalogue will be delivered at the end of 2018.

A workshop has been organized (November 21st-23rd) in Potsdam («Workshop European seismology at the frontier: new capabilities and techniques. Potsdam November 21-23»). New types of seismological instrumentation (fiber optics, rotational sensors, massive devel-

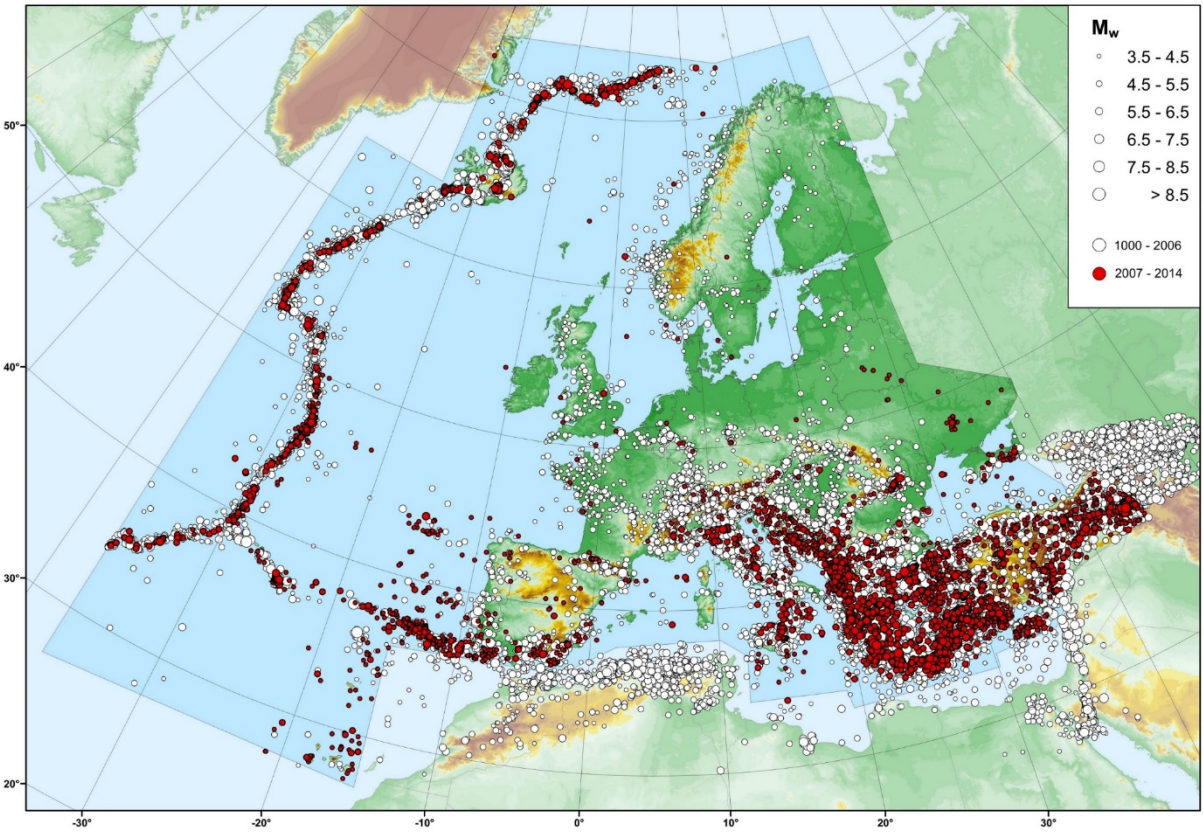

Figure 13. New events (red) in the 2007–2014 period compared with the previous EMEC catalogue (white).

opment of low-cost sensors) and computing opportunities will be widely available in upcoming years. The goal of the workshop will be to evaluate the immediate impact of new techniques and the expected long-term science evolutions that cross the boundaries of traditional seismological research. We will address the problem of actual and future network performance and of the influence of the network characteristics (geometry, instrumentation) on the physical and statistical understanding of earth processes. Several concise presentations including at least two focusing on broader impacts, will be followed by brain storming discussions aiming at addressing questions about emerging science opportunities, required facilities, and broader impacts. We expect the following deliverables from the meeting:

- a priority list of the analyses which should be performed to test European key seismic networks and their potential future configurations;

- a white paper delivering guidance for European seismological networks improvement (or redesign) and highlighting new capabilities, beyond those that might presently exist, which will be required to make rapid progress in addressing one or more science grand challenge questions.

7 References

Aiken, J. M., C. Aiken, and F. Cotton (2018): A Python library for teaching computation to seismology students, Seismological Research Letters, Vol. 89, No. 3, p. 1165–1171.

Broccardo, M., A. Mignan, S. Wiemer, B. Stojadinovic, and D. Giardini (2017), Hierarchical Bayesian Modeling of Fluid-Induced Seismicity, Geophys. Res. Lett., 44(22), 11357-11367, doi:10.1002/2017gl075251.

Burkhard, M., and G. Grünthal (2009): Seismic source zone characterization for the seismic hazard assessment PEGASOS by the Expert Group 2 (EG1b), Swiss Journal of Geosciences, Vol. 102, p. 149–188.

Grasso, J.-R., A. Karimov, D. Amorese, C. Sue, and C. Voisin (2018): Patterns of reservoir-triggered seismicity in a low-seismicity region of France, Bulletin of the Seismological Society of America, doi: https://doi.org/10.1785/0120180172

Grünthal, G., and R. Wahlström (2012): The European-Mediterranean Earthquake Catalogue (EMEC) for the last millennium, Journal of Seismology, Volume 16, No. 3, p. 535-570.

Helmstetter, A., Y. Y. Kagan, and D. D. Jackson (2007): High-resolution time-independent grid-based forecast for M ≥ 5 earthquakes in California, Seismological Research Letters, Vol. 78, No. 1, p. 78–86.

Lammers S., D. Stromeyer, G. Weatherill, F. Cotton, and G. Grünthal (2018): Towards a New Harmonised Earthquake Catalogue for the Euro-Mediterranean Region, Paper presented at European Geosciences Union General Assembly 2018, Vienna/Austria, 8-13 April 2018 (Geophysical Research Abstracts, Vol. 20, EGU2018-12225)

Kiraly-Proag, E., J. D. Zechar, V. Gischig, S. Wiemer, D. Karvounis, and J. Doetsch (2017), Validating induced seismicity forecast modelsInduced Seismicity Test Bench, J Geophys Res-Sol Ea, 121(8), 6009-6029

Kiraly-Proag, E., V. Gischig, J. D. Zechar, and S. Wiemer (2018), Multicomponent ensemble models to forecast induced seismicity, Geophys. J. Int., 212(1), 476-490, doi:10.1093/gji/ggx393.

Mignan, A., M. Broccardo, S. Wiemer, and D. Giardini (2017), Induced seismicity closed-form traffic light system for actuarial decision-making during deep fluid injections, Sci Rep-Uk, 7

Marzocchi, W. and M. Taroni (2014): Some thoughts on declustering in probabilistic seismic-hazard analysis, Bulletin of the Seismological Society of America, Vol. 104, No. 4, p. 1838–1845.

Nandan, S., G. Ouillon, S. Wiemer, and D. Sornette (2017): Objective estimation of spatially variable parameters of epidemic type aftershock sequence model: application to California, Journal of Geophysical Research: Solid Earth, Vol. 122, p. 5118–5143.

Taroni, M., W. Marzocchi, D. Schorlemmer, M. J. Werner, S. Wiemer, J. D. Zechar, L. Heiniger, and F. Euchner (2018), Prospective CSEP Evaluation of 1-Day, 3-Month, and 5-Yr Earthquake Forecasts for Italy, Seism. Res. Lett., 89(4), 1251-1261, doi:10.1785/0220180031.

Stallone, A. and W. Marzocchi (2018a, in review): Empirical evaluation of the magnitude-independence assumption, submitted to Geophysical *Journal International*.

Stallone, A. and W. Marzocchi (2018b, in review): Features of seismic sequences are similar in different crustal tectonic regions, *submitted to Bulletin of the Seismological Society of America*.

Schorlemmer, D., et al. (2018), The Collaboratory for the Study of Earthquake Predictability: Achievements and Priorities, Seism. Res. Lett., 89(4), 1305-1313, doi:10.1785/0220180053.

Woessner, J., D. Laurentiu, D. Giardini, H. Crowley, F. Cotton, G. Grünthal, G. Valensise, R. Arvidsson, R. Basili, M. B. Demircioglu, S. Hiemer, C. Meletti, R. W. Musson, A. N. Rovida, K. Sesetyan, M. Stucchi, and the SHARE Consortium (2015): The 2013 European seismic hazard model: key components and results, *Bulletin of Earthquake Engineering*, Vol. 13, No. 12, p. 3553–3596.

Zaliapin (2008)

Upcoming publications: new EMEC catalog for Europe (Graeme and Steffi), SERA background seismicity paper,

SERA Project Office | ETH Department of Earth Sciences
Sonneggstr. 5, NO H-floor, CH-8092 Zurich | sera_office@erdw.ethz.ch | +41 44 632 9690 |
www.sera-eu.org